



Interaction between lakes' surface water and groundwater in the Pantanal wetland, Brazil

J. G. Freitas¹ · S. A. C. Furquim¹ · R. Aravena² · E. L. Cardoso³

Received: 26 April 2018 / Accepted: 15 February 2019 / Published online: 22 February 2019
© Springer-Verlag GmbH Germany, part of Springer Nature 2019

Abstract

The Nhecolândia subregion (area ~ 26,921 km²), in central-southern Pantanal, is marked by the presence of hundreds of alkaline–saline lakes, located on the top of sand hills, and thousands of non-alkaline lakes adjacent to the sand hills. This study aimed to provide a better understanding of the hydrological dynamics in the Nhecolândia, which is scarce and controversial, based on piezometric monitoring, isotopic data and chemical analyses of the surface water and groundwater of an alkaline–saline lake, a non-alkaline lake and the sand hill between them. The potentiometric data indicated that both alkaline–saline and non-alkaline lakes act as recharge zones, the former in all seasons and the later only in the wet season. These results are corroborated by downward flow near the zones of recharge, indicated by hydraulic head measurements in multilevel wells around the non-alkaline lake and in mini-piezometers installed in the studied alkaline–saline lake and two more lakes in the region. Also, $\delta^{18}\text{O}$ and $\delta^2\text{H}$ values of the alkaline–saline lake surface water became more depleted than the surrounding groundwater in the wet season, confirming that the inflow to the alkaline–saline lake in this season was by the more depleted rainwater and not by the isotopically enriched groundwater. The water chemistry data is also in agreement with recharge from the alkaline–saline lake, even though this recharge is limited by a low-K layer. Because of this layer, the non-alkaline lake does not dry off during the dry season. This set of evidence demonstrated that the groundwater recharge in the study area occurs in the topographical lows, through a process known as depression-focused recharge, which disagrees with previous studies of the area.

Keywords Groundwater–surface water interaction · Wetland · Depression-focused recharge

Introduction

The Pantanal wetland is an active Cenozoic sedimentary basin located in the central zone of South America (16°–20°S and 58°–50°W), mostly in Brazil (90%), but also in small areas of Bolivia and Paraguay (10%) (Padovani 2010; Assine et al. 2015) (Fig. 1). The region is mainly

formed by alluvial fans, floodplains and lacustrine depositional systems (Assine 2003; Assine et al. 2015) and is characterized by extremely low slope gradients (<1%) and altitudes between 100 and 200 m (Silva 1986; Scott 1991). It is one of the largest complexes of wetlands in the world (area ~ 150,500 km²), with still pristine ecosystems and large plant and animal diversity (Silva et al. 2001; Junk et al. 2006). These features qualify the region as a World Heritage Area by UNESCO and a wetland of international importance by the Ramsar Convention of Wetlands.

The main watercourse of the wetland is the Paraguay river, an important tributary of the La Plata basin, which is the fifth largest drainage system in the world (area ~ 3.2 million km²) (Collischonn et al. 2001; Berbery and Barros 2002). The Pantanal is specifically located in the Upper Paraguay basin (area ~ 496,000 km²), the uppermost region of the Paraguay drainage system, situated upstream the confluence between the Apa and Paraguay rivers (Cordeiro 1999) (Fig. 1). The Upper Paraguay basin also comprises

✉ S. A. C. Furquim
sacfurquim@gmail.com

¹ Department of Environmental Sciences, Universidade Federal de São Paulo (UNIFESP), Rua São Nicolau, 210, Centro, Diadema, São Paulo 09913-030, Brazil

² Department of Earth and Environmental Sciences, University of Waterloo, 200 University Ave. W, Waterloo, ON N2L3G1, Canada

³ Empresa Brasileira de Pesquisas Agropecuárias, EMBRAPA, Corumbá-MS, Rua 21 de Setembro, 1880, Aeroporto, Corumbá, Mato Grosso do Sul 79320-900, Brazil

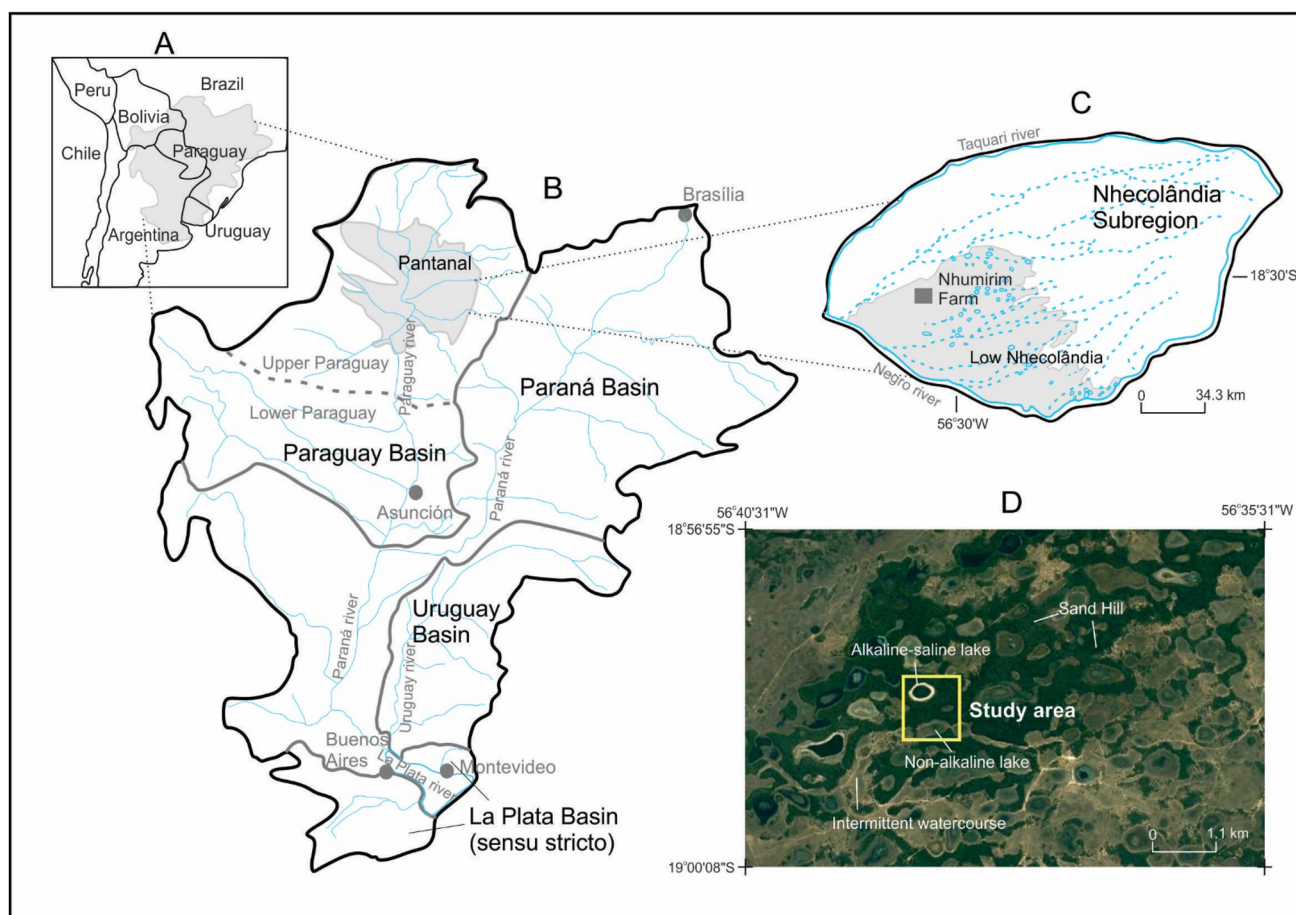


Fig. 1 **a** Location of the La Plata basin in South America (adapted from: FAO-AQUASTAT 2016); **b** La Plata Basin (sensu lato) and location of the Pantanal wetland (adapted from: OEA 2017; FAO-AQUASTAT 2016); **c** Nhecolândia subregion and location of the

Nhumirim Farm, where the study was conducted (adapted from: Fernandes et al. 1999; Capellari 2001); **d** aerial photography of the Nhumirim Farm, with the study area and surroundings (adapted from: Google Earth 2017)

the highlands that surround the Pantanal, formed by escarpments and hills with altitudes between 200 and 900 m and by Precambrian crystalline and Mesozoic sedimentary rocks. The headwaters of the Paraguay river and tributaries are mainly located in these highlands, which provide an important supply of water and sediments to the wetland during the seasonal floodings (Del'Arco et al. 1982; Alvarenga et al. 1984; Godoi Filho 1986; Por 1995).

A time lag of 2–3 months generally occurs between the beginning of the rainy season and the start of the flooding in the Pantanal (Padovani 2010). The inundation pulse takes 4–6 months to cross the wetland, reaching its maximum at February–March in the northern and eastern and at June–July in the southernmost subregions, already in the dry season (Carvalho 1986; Hamilton et al. 1996; Padovani 2010). During a calendar year, the maximum area subjected to inundation is of approximately 131,000 km² and the maximum area that is simultaneously flooded is about 110,000 km² (Hamilton et al. 2002). The main processes that

trigger inundation are the water discharge from the channel to the floodplain, the slowness or prevention of the drainage of the floodwater due to the inundation of the Paraguay river and the accumulation of water from local precipitation, mainly in areas that are away from the main rivers (Hamilton 1999).

The Nhecolândia (area ~26,921 km²), a subregion located in the central-southern Pantanal (Fig. 1), corresponds to the south part of the Taquari alluvial fan, which has a rounded shape and a huge size, with a diameter of ~250 km and an area of ~49,000 km² (Zani et al. 2006, 2012). Sandy sediments have been deposited in the Taquari megafan since the Pleistocene, being mostly composed of quartz, but with minor amounts of more weatherable minerals, such as microcline and albite (Furquim 2007; Zani et al. 2012). The source area of these sediments is the Paleozoic sandstones of the Paraná basin located mainly in the Serra de Maracajú, a dissected highland that surrounds the west side of the Pantanal. The megafan is formed by a modern lobe near the

Taquari river, where the sedimentation is active, and five abandoned lobes marked by preserved paleochannels and current erosional features. The Nhecolândia is mainly situated in the two oldest abandoned lobes (Zani et al. 2006).

Because of the relatively higher altitudes of the Nhecolândia if compared with other areas of Pantanal, the flooding in this subregion is not directly affected by the level of the nearest main rivers (Taquari, Negro or Paraguay rivers) and the most important contribution for the floodwaters comes from local precipitation (Costa et al. 2015; Hamilton 1999). Approximately, 45–50% of its area does not inundate, about 40% remain inundated only up to 10% of the time and less than 1% is permanently flooded. In the low Nhecolândia (Fig. 1), a zone within the subregion with relatively lower altitudes, the peak of the inundation varies from February to May, with an area of flooding close to 4,000 km² in each of these months and a general floodwater flow with NE–SW direction (Padovani 2010; Hamilton et al. 1996).

Important landscape features of the low Nhecolândia (area ~ 8,220 km²) (Fig. 1) are the occurrence of about 640 alkaline–saline lakes and 8200 non-alkaline lakes (Costa et al. 2015). Despite being closely located, there is a great contrast in water quality between these lakes, with the alkaline–saline lakes presenting pH higher than 8.0, electrical conductivity higher than 5 mS cm⁻¹, and high concentration of bicarbonate, sodium and potassium. On the other hand, in the non-alkaline lakes, pH is lower than 7 and the electrical conductivity is commonly less than 1 mS cm⁻¹ (Almeida et al. 2003). The alkaline–saline lakes are rounded depressions that hardly dry off, with 0.5–1 km in diameter and 2–5 m in depth. They are located on the top of sand hills, which are narrow (200–300 m wide) sandy stripes 2–5 m higher than the surroundings, representing the highest topographical level of the region. This slight altitudinal gradient prevents the floodwater input, allowing the presence of forested savanna vegetation in the sand hills and around the saline lakes. The non-alkaline lakes are temporary waterbodies located in the lowest zones, with different forms and dimensions and up to 2 m depth. During the peak of seasonal inundation, the non-alkaline lakes merge and form intermittent watercourses, which can have 30 m of width and long extensions (Barbiero et al. 2002). Open grass savanna and swampy grasslands are the dominant vegetation in the complex non-alkaline lakes/intermittent watercourses (Evans and Costa 2013).

Although important knowledge about the regional flooding in the Pantanal and Nhecolândia is available in the literature, detailed information about the hydrological functioning of alkaline–saline lakes/sandy hills and non-alkaline lakes/intermittent watercourses complexes is still scarce, being mainly based on landscape elements, with no or a few field hydrological measurements. Barbiero et al. (2008) proposed a hypothesis of hydrologic functioning supported mainly by

soil morphological data and water level measurements along one transect. The soil morphology under and around the alkaline–saline lakes is mainly formed by a dark and loamy sand horizon in the surface (*H*), followed in depth by grayish and sand to loamy sand horizons (*E*, *Bkg*¹), which overlay a greenish, sandy loam and nearly impervious horizon (*Bnq*²) (Furquim 2007; Barbiero et al. 2008). Barbiero et al. (2008) observed that the *Bnq* completely surrounds the lake, being responsible for retaining the subsurface water in the saline depression during part of the year. During the wet season, the subsurface water level would rise and move from the non-alkaline lakes/intermittent watercourses to the saline lakes, passing over the low permeable *Bnq*. However, during the dry season, the water level would drop and the *Bnq* horizon would act as a barrier to the return flow from the alkaline–saline lake to the non-alkaline lakes/intermittent watercourses, providing a seasonal retention of the subsurface water.

Costa et al. (2015) suggested a different hypothesis, based on topographical data extracted from satellite images. During the wet season, the sandy hills would act as a recharge zone, with the groundwater flowing from the highest topographical zones to the adjacent non-alkaline and alkaline–saline depressions. This behavior would be responsible for the alkaline–saline lake isolation during part of the year, without any kind of barrier, suggesting that the low permeable horizon (*Bnq*) that surrounds these lakes are more likely the consequence than the cause of the hydrological functioning. During the dry season, however, the water level elevation would decrease, stopping the flows from the highest zones. During this period, the subsurface flow would occur from the non-alkaline lake/intermittent watercourse to the saline lake, inasmuch as the bottom of the latter is usually 0.5–1.5 m lower than the bottom of the former. According to this statement, the alkaline–saline lake would receive subsurface water during the whole year, preventing its full drying most of the time.

Several methods can be applied to understand the hydrology and connection between surface water and groundwater in wetlands. Piezometric monitoring of hydraulic heads is commonly used to map the direction of flow (Bradley et al. 2007; Rosenberry et al. 2015; Kebede et al. 2016). It is usually combined with other techniques, such as hydrochemical and stable isotopic monitoring (Montalván et al. 2017; Kebede et al. 2016; Rosenberry et al. 2015; Bradley et al. 2007). Oxygen and hydrogen isotopes are particularly useful

¹ The suffixes *k* and *g* indicate, respectively, carbonates accumulation and iron reduction due to prolonged soil saturation (Schoeneberger et al. 2012).

² The suffixes *n* and *q* indicate, respectively, accumulation of pedogenic exchangeable sodium and accumulation of pedogenic silica (Schoeneberger et al. 2012).

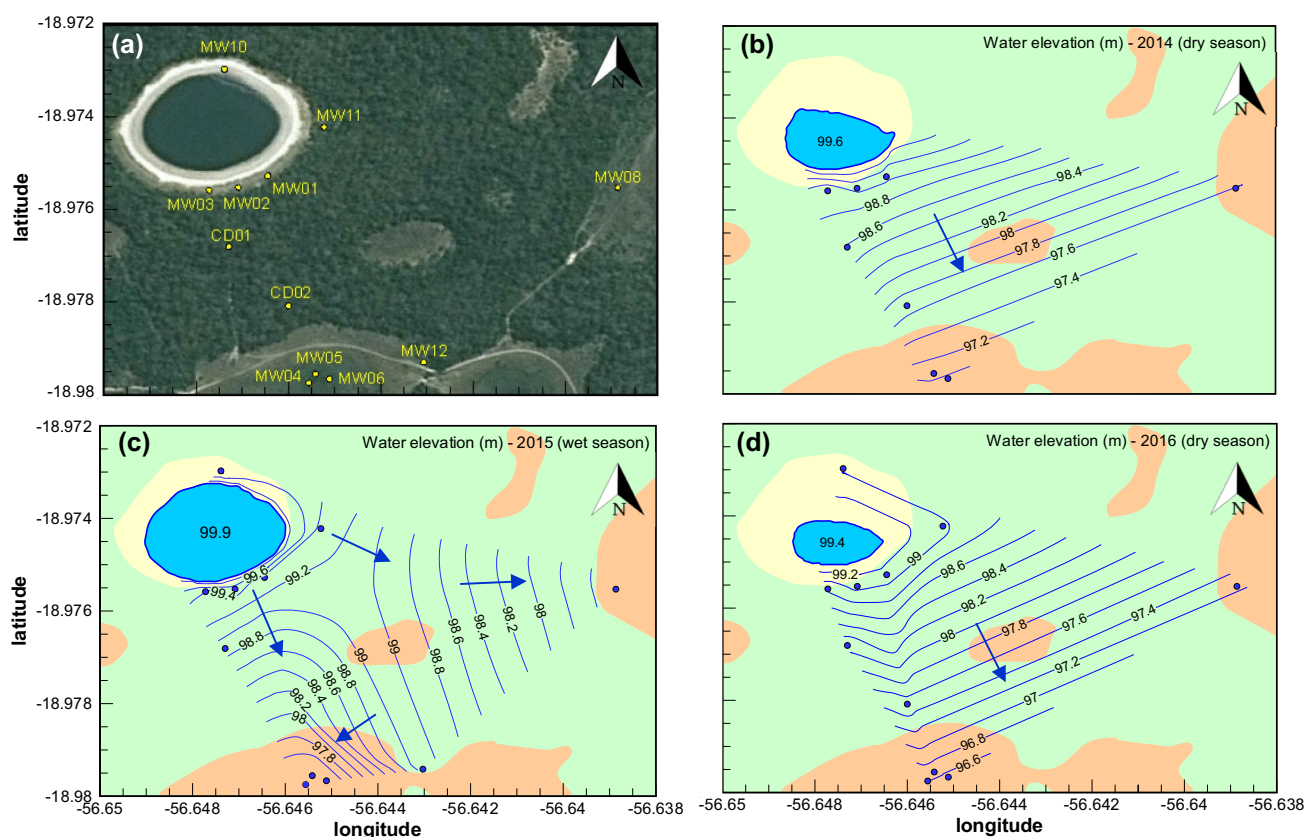


Fig. 2 Monitoring wells' location (**a**, yellow circles) and potentiometric surfaces in three monitoring events (**b–d**). Multilevel wells have two levels at the same coordinates and are represented as one circle.

On Fig. 2b–d, only the wells with available data at the monitoring event are indicated (blue circles). Blue lines represent equipotential curves and blue arrows indicate main flow directions

since they are ideal tracers, not dissolved solutes (Rosenberry et al. 2015).

Regarding the controversial explanations, the objective of this work is to provide a better understanding of the hydrological dynamics in the low Nhecolândia, through piezometric monitoring, isotopic and chemical data, specifically focusing on the variability of the subsurface flow directions along the year, the genesis of the waters and the interactions between surface and subsurface waters.

Materials and methods

Site monitoring

A total of fifteen 2" groundwater monitoring wells were installed from Oct. 2014 to Apr. 2015; six were located around a representative alkaline–saline lake (SL), two on the adjacent sand hill (SH), one in the border of a slightly depression within the sand hill and six around a nearby non-alkaline lake (NAL) (Fig. 2). Monitoring wells MW 02, 05 and 06 were multilevel. The location of the monitoring wells

was based on the regional groundwater flow direction, from NE to SW (Padovani 2010). Wells' geometry is presented on Table 1. Depth to water table was monitored manually every 2 weeks from Oct. 2014 to Aug. 2015 and in a separate event in Oct. 2016 (dry season). The non-alkaline lake water column is around 0.4 m (Barbiero et al. 2018). The water level in the alkaline–saline lake was monitored on three dates: Oct. 2014, Apr. 2015 and Oct. 2016.

Two water sampling events were conducted, the first in Oct. 2014, in the dry season, and the second in Apr. 2015, in the wet season. During each event, field measurements were performed for pH, electrical conductivity (EC), oxidation–reduction potential (ORP) and dissolved oxygen (DO) in groundwater and surface water from the alkaline–saline lake. Surface water from the non-alkaline lake was not sampled, since it had no water in the dry season and only a few centimeters of water during the wet season sampling event. Groundwater and surface water were sampled for chemical and stable isotope ($\delta^{18}\text{O}$, $\delta^2\text{H}$) analysis. Chemical parameters analyzed were anions Cl^- , SO_4^{2-} , NO_3^- , PO_4^{3-} , F^- , Br^- and cations Na^+ , Ca^{2+} , Fe^{2+} , Mg^{2+} , Al^{3+} , K^+ . Bicarbonate concentration was estimated

Table 1 Monitoring wells (MW and CD) and mini-piezometers' (MPZ) properties

	Location	Coordinates		Ground elevation (m)	Depth (m)	Screen length (m)	Date installed
		S	W				
MW01	Alkaline–saline lake	18°58'31.0"	56°38'47.2"	100.33	1.88	0.20	10/10/2014
MW2A	Alkaline–saline lake	18°58'31.9"	56°38'49.5"	100.25	2.00	0.20	11/10/2014
MW2B	Alkaline–saline lake	18°58'31.9"	56°38'49.5"	100.29	1.68	0.20	11/10/2014
MW03	Alkaline–saline lake	18°58'32.1"	56°38'51.8"	100.22	1.59	0.20	11/10/2014
MW04	Non-alkaline lake	18°58'47.1"	56°38'44"	99.19	3.94	0.20	12/10/2014
MW05A	Non-alkaline lake	18°58'46.1"	56°38'43.5"	99.67	5.97	0.50	13/10/2014
MW05B	Non-alkaline lake	18°58'46.1"	56°38'43.5"	99.66	3.77	0.50	13/10/2014
MW06A	Non-alkaline lake	18°58'46.8"	56°38'42.4"	99.28	6.12	0.50	13/10/2014
MW06B	Non-alkaline lake	18°58'46.8"	56°38'42.4"	99.24	4.07	0.50	13/10/2014
MW08	Border of slight depression	18°58'31.9"	56°38'19.9"	100.89	4.25	0.50	17/10/2014
CD1	Sand hill	18°58'37.6"	56°38'50.0"	103.34	5.65	0.50	15/10/2014
CD2	Sand hill	18°58'41.1"	56°38'45.6"	102.45	5.55	0.50	16/10/2014
MW10	Alkaline–saline lake	18°58'22.7"	56°38'50.6"	100.07	2.09	0.50	11/04/2015
MW11	Alkaline–saline lake	18°58'27.2"	56°38'42.82"	100.72	1.89	0.50	11/04/2015
MW12	Sand hill	18°58'45.9"	56°38'34.9"	101.81	2.92	0.50	12/04/2015
MPZ-14	Alkaline–saline lake	18°58'29.7"	56°38'51.8"	–	0.30	0.10	31/10/2014
MPZ1-15	Alkaline–saline lake	18°58'25.2"	56°38'50.5"	–	0.13	0.10	11/04/2015
MPZ2-15	Alkaline–saline lake	18°58'27.3"	56°38'47.0"	–	0.15	0.10	11/04/2015
MPZ3-15	Alkaline–saline lake	18°58'30.5"	56°38'51.0"	–	0.21	0.10	11/04/2015
MPZ1-16	Alkaline–saline lake	18°58'29.7"	56°38'50.6"	–	0.50	0.10	01/10/2016
MPZ2-16	Alkaline–saline lake	18°58'28.6"	56°38'48.2"	–	0.34	0.10	01/10/2016
MPZ3-16	Alkaline–saline lake	18°58'29.5"	56°38'53.3"	–	0.36	0.10	01/10/2016
MPZ4-16	Alkaline–saline lake	18°58'27.2"	56°38'51.9"	–	0.46	0.10	01/10/2016
MPZ5-16	Alkaline–saline lake (salina do 8)	18°58'59.3"	56°39'48.1"	–	0.50	0.10	04/10/2016
MPZ6-16	Alkaline–saline lake (reserva)	18°57'35.6"	56°37'19.7"	–	0.21	0.10	04/10/2016

based on ionic balance. Groundwater was sampled with a peristaltic pump by low-flow pumping, filtered and acidified to $\text{pH} < 1.5$ for cations analyses and frozen for anions analyses. Analytical methods are presented in “Analytical methods”.

Rain water and surface water (alkaline–saline lake) were also sampled monthly during the wet season (Dec. 2014 to Mar. 2015). Precipitation samples were collected from a rain gauge installed approximately 2 km away from the field site, as aliquots of the total month precipitation. Samples were analyzed for $\delta^{18}\text{O}$ and $\delta^2\text{H}$.

Mini-piezometers were installed within the alkaline–saline lake approximately 30 cm below lakebed for hydraulic head monitoring (Lee and Cherry 1978) (Table 1). Piezometers were constructed with transparent polyethylene tubing, 1/8" ID, perforated in the bottom 10 cm and covered with a 177 μm nylon mesh (ASTM 80). Mini-piezometers were also installed in two other alkaline–saline lakes in Oct. 2016 outside the study area, to verify if the observed behavior was common to other alkaline–saline lakes in the region.

Analytical methods

Quantification of Al^{3+} , Ca^{2+} , Mg^{2+} and Fe^{2+} was performed by inductively coupled plasma optical emission spectrometry (ICP-OES) (Varian 720-ES), at the CEPEMA-USP Laboratory. Samples were digested with concentrated nitric acid following USEPA Method 3015A (2007). Na^+ and K^+ were determined by flame photometry (Flame photometer DM-62, Digimed), at UNIFESP. Anions were quantified by ion chromatography (Bioagri Laboratory), following method USEPA 300.1 (1999). Quantification limits ranged from 0.005 to 100 mg L^{-1} . Isotopes ($\delta^{18}\text{O}$ and $\delta^2\text{H}$) were determined at the Environmental Isotope Laboratory, at the University of Waterloo by laser absorption with a Los Gatos Research OA-ICOS T-LWIA.

Results and discussion

Potentiometry

Potentiometric surfaces were constructed for three monitoring events, for the dates on which the level on the alkaline–saline lake was also measured (Oct. 2014, Apr. 2015 and Oct. 2016) (Fig. 2). The alkaline–saline lake area varied significantly between the wet and dry seasons, due to the high evaporation and relatively flat topography. The potentiometric maps indicate a main component of groundwater flow from NNW to SSE on the dry seasons (Fig. 2b and d), indicating a deviation from the regional groundwater flow. The alkaline–saline lake presented higher elevation than the surrounding groundwater in all monitoring events, indicating that the lake does not receive groundwater discharge, but acts as a recharge zone. However, the hydraulic conductivity (K) of the subsurface horizon Bnq is low (in the order of 10^6 m s^{-1}), mainly due to the cementation of sand, silt and clay particles by amorphous silica and the consequent obstruction of the porosity (Furquim 2007; Damaceno et al., in submission). Thus, the water infiltration is low in the lake depression, resulting in water accumulation within the lake throughout the year.

During the wet season, the potentiometric surface indicated different flow components (Fig. 2c). In the northern part of the study area, groundwater initially flows from NW to SE from the alkaline–saline lake region, and becomes approximately W to E oriented towards the eastern section of the study area. In the non-alkaline lake region, two water flow directions converge, one from the alkaline–saline lake (flowing NNW to SSE) and another starting approximately in the middle of the site (NE to SW). The occurrence of groundwater flowing to two different directions (W–E and NE–SW) indicates the presence of a recharge zone. This behavior is likely associated with a non-vegetated depression zone located approximately in the middle of the site (lat.: -18.977 ; long.: -56.644). During the wet season, this slight depression can accumulate water and recharge the groundwater, acting also as a local recharge zone, in the same manner as described by Furian et al. (2013) for an oligosaline pond in the Nhecolândia subregion. Unfortunately, it was not possible to install monitoring wells on the area of this depression due to access limitations.

During the monitored period, the highest air temperature was $41.4 \text{ }^\circ\text{C}$, recorded in Sep 30, 2016, and the lowest was $7.0 \text{ }^\circ\text{C}$, in July 2016. In the same period, monthly precipitation reached a maximum of 260 mm, in Jan. 2016. In general, greater precipitation events were focused between Nov. and Jan., during the wet season (Fig. 3). The water table in all monitoring wells varied similarly, showing an

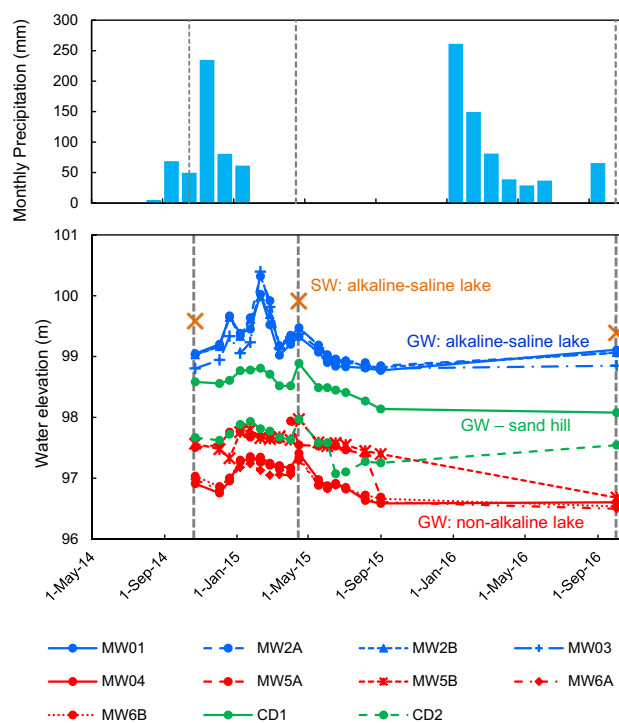


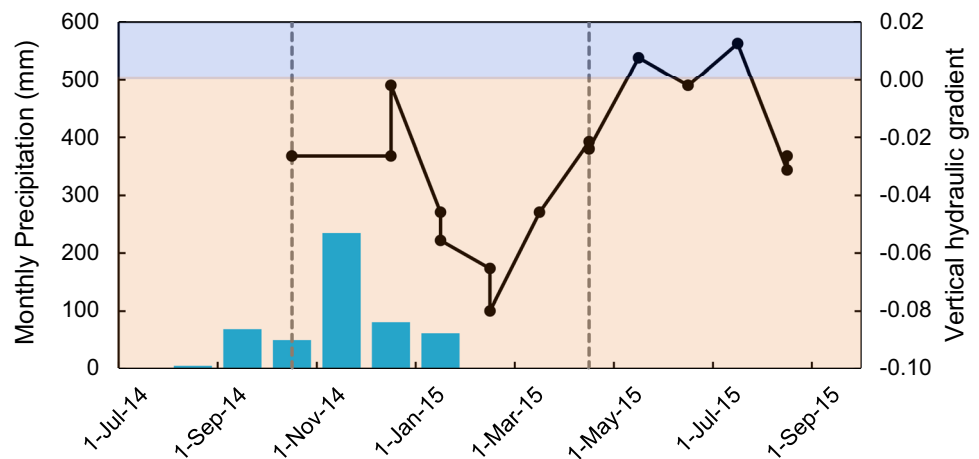
Fig. 3 Groundwater (GW) and surface water (SW) elevation temporal variation. Dashed gray lines indicate sampling events

increase in elevation following precipitation, caused by recharge from upgradient in the study area and in depression zones. However, greater oscillations in groundwater level were measured in alkaline–saline lake wells, likely due to the closer positioning to the alkaline–saline lake, which acts as a recharge zone. The depth to the water table around the alkaline–saline lake ranged from 0.4 m bgs (below ground surface) in MW2B in the wet season (Feb. 2015) to 1.73 m bgs in MW01 in the dry season (end of Aug. 2015).

Over time, the groundwater levels close to the alkaline–saline lake were always higher than the sand hill and non-alkaline lake wells (Fig. 3), indicating that the behavior observed during the three sampling events previously described continued during the year, with groundwater flow direction occurring from NNW to SSE. During a short period, of approximately 2 months, one well in the non-alkaline lake surroundings (MW05B) presented higher water elevation than the wells located in the sand hill. This could be an effect of faster water uptake by the deep rooted forested savanna vegetation in the sand hill, causing a faster drop in water level during the dry season (Zevenbergen 2012).

The multilevel well in greater proximity to the saline lake (MW02) did not indicate a significant vertical gradient, indicative of predominant horizontal flow. Mini-piezometers installed in the alkaline–saline lake sediments presented hydraulic gradient indicative of downwards flow, ranging

Fig. 4 Relation between monthly precipitation (blue columns) and groundwater vertical hydraulic gradient in the non-alkaline lake (MW06) (black line). Negative hydraulic gradient values indicate downwards flow



from 0.27 to 0.02 m m^{-1} . The hydraulic head measurements performed in mini-piezometers in two other alkaline–saline lakes in Oct. 2016 also indicated downwards flow, suggesting that alkaline–saline lakes recharging groundwater is typical for alkaline–saline lakes in the region.

Concerning the non-alkaline lake, the vertical hydraulic gradient in the multilevel wells close to the non-alkaline lake indicated a predominance of downwards flow throughout the year, indicating that the non-alkaline lake is not a discharge zone, but is also a recharge area (Fig. 4). The magnitude of the vertical hydraulic gradient close to the non-alkaline lake increased as the wet season progressed, likely due to the increased water accumulation in the lake, which caused it to act as a local recharge zone in the wet season. In the dry season, the magnitude of the vertical hydraulic gradient decreased, and the flow became predominantly horizontal.

Water chemistry

Groundwater and surface water in the study area are predominantly sodium-bicarbonate-type water characterized by different degrees of salinization (Table 2). The conductivity data show a wide range of values without any significant difference between the dry and wet season. The highest degree of salinity in water is represented by the groundwater in the alkaline–saline lake area which are characterized by values between 27 and 12 mS cm^{-1} and the lowest degree of salinity in water is represented by the groundwater in the sand hills and non-alkaline lake area with values between 0.1 and 1.2 mS cm^{-1} . The alkaline lake water shows conductivity values of 3.5 (rainy season) and 5.9 (dry season) mS cm^{-1} . The electrical conductivity values measured in the surface water are in the range of very high salinity to hypersaline water, according to Almeida et al. (2010). The values obtained were higher than reported by Barbiero et al. (2018) for Dec. 2014 and Jul. 2015 (around 2 mS cm^{-1}). However, previous research by Barbiero et al. (2002) reported higher

ions concentrations in the alkaline–saline lake surface water during the dry season than the values found in this study (Table 2). Cl^- concentrations were two orders of magnitude higher, SO_4^{2-} one order of magnitude, and Na^+ , Mg^{2+} and K^+ approximately five times higher (Barbiero et al. 2002). The lower values observed could be partially attributed to rainfall that occurred previously to the sampling events. The 2014 wet season started early, with some rains recorded as early as August. Therefore, during the sampling in the 2014 dry season, some rainfall events had occurred, which could have resulted in surface water dilution. The isotope data discussed in the next section show extremely enriched values during the dry compared to the wet season typically associated with greater evaporation during the dry season. Considering that the isotope measurements and EC value are in the range expected, it is also possible that there was some analytical error in the anions' quantification.

Barbiero et al. (2002) indicated that the evaporation of subsurface freshwater is the main process responsible for higher ions' concentration in the ground and surface water associated with the alkaline–saline lakes of Nhecolândia, compared with the water of the sand hills and non-alkaline lakes. However, the other hypothesis that is examined in our study is that the salinity of the groundwater in the alkaline lake area is partly associated with dissolution of salt in the sediments near the lake.

The water chemistry in the alkaline–saline lake is associated with transport of chemical elements by rainwater, runoff and shallow subsurface flow through the sand to loamy sand horizons (E, Bkg) above the low-K horizon (Bnq), allowing the dissolution of minerals and transport to the alkaline–saline lake, where the concentrations increase due to the evaporation process. The sand and silt fractions of these sandy horizons above the Bnq are mainly composed by quartz (SiO_2), but feldspars such as microcline (KAlSi_3O_8) and albite ($\text{NaAlSi}_3\text{O}_8$) are also present (Furquim 2007). In the alkaline conditions prevalent in the soils around the

Table 2 Chemical and stable isotopic data

Monitoring well	pH	EC mS cm ⁻¹	Eh mV	$\delta^{18}\text{O}$ ‰	$\delta^2\text{H}$	DO mg L ⁻¹	Cl ⁻	SO ₄ ²⁻	NO ₃ ⁻	PO ₄ ³⁻	F ⁻	Br ⁻	HCO ₃ ⁻	Na ⁺	Ca ²⁺	Fe ²⁺	Mg ²⁺	Al ³⁺	K ⁺
2014—dry season																			
Monitoring wells around the alkaline-saline lake																			
MW01	9.60	18.1	-286	0.98	-7.16	0.24	1720	169	<50	109	<5	7.1	16,600	6720	22.6	0.79	1.04	<0.05	1320
MW2A	10.0	16.1	-392	0.82	-7.45	0.31	1090	91.1	<50	41.1	<5	4.4	10,020	4030	13.4	0.59	0.78	<0.05	872
MW2B	9.16	12.4	-310	-0.43	-11.6	0.00	540	42.5	<25	23.9	<2.5	2.2	9330	3430	10.8	0.57	0.82	<0.05	786
MW03	10.3	19.9	-306	0.39	-7.41	0.57	1450	155	<100	74.8	<10	6	21,700	8230	NA	6.61	11.1	<0.05	1670
Monitoring wells around the non-alkaline lake																			
MW04	6.57	1.12	60.0	-2.17	-20.2	1.03	0.77	3.23	<0.5	0.67	<0.05	0.01	817	184	43.4	11.1	12.9	<0.05	73.1
MW05A	6.60	0.41	50.0	-1.44	-18.2	0.79	3.96	0.98	<0.5	0.71	0.31	0.02	310	79.7	7.15	6.21	3.16	<0.05	37.4
MW05B	6.07	0.55	105	-1.51	-17.2	NA	3.14	2.7	<0.5	0.83	0.39	0.03	202	62.4	0.95	0.45	0.71	<0.05	26.4
MW06A	6.43	0.89	64.0	-2.54	-22.8	0.47	5.39	9.63	<0.5	0.48	<0.05	0.04	474	115	22.2	3.72	5.21	<0.05	56.7
MW06B	6.50	0.96	-4.00	-2.59	-22.7	0.82	7.80	23.9	<1	0.29	<0.1	0.07	552	151	22.8	1.91	6.14	<0.05	58.8
MW08	6.60	0.87	-71.0	-0.93	-14.0	0.59	12.1	<1	<1	<0.1	<0.1	0.05	456	117	19.3	1.01	6.83	<0.05	45.7
Monitoring wells in the sand hill																			
CD1	6.31	0.14	-35.0	-4.28	-30.9	0.20	1.42	<0.5	<0.5	0.28	<0.05	0.01	77.8	9.60	6.43	3.63	1.49	<0.05	13.0
CD2	6.26	NA	-61.0	-1.68	-18.2	0.95	1.42	<0.5	<0.5	0.28	<0.05	0.01	63.2	11.6	1.20	1.35	0.82	<0.05	15.8
Alkaline-saline lake surface water																			
SW	9.39	5.90	6.50	14.1	71.15	4.57	16.7	48.3	28.6	<0.05	<0.05	0.07	4180	1360	4.70	1.5	0.88	<0.05	424
2015—wet season																			
Monitoring wells around the alkaline-saline lake																			
MW01	9.91	27.0	-276	0.66	-7.64	1.45	1510	157	<0.015	31.5	1.5	3.79	22,200	8390	4.85	24.2	1.23	10.49	1690
MW2A	9.66	17.5	-250	0.65	-7.09	0.88	590	39.4	0.16	8.14	0.29	1.34	10,900	3980	1.42	0.59	1.43	0.94	873
MW2B	9.60	13.9	-173	0.01	-11.3	1.16	208	21.4	0.14	3.05	0.24	0.56	9220	3190	3.36	0.33	1.37	0.49	723
MW03	9.83	20.0	-224	0.83	-6.66	1.18	1060	102	0.62	18.9	1.25	2.75	15,300	5820	1.76	1.41	12.4	0.37	1130
MW10	9.78	19.9	-168	0.97	-6.53	1.43	719	53.4	0.66	10.9	1.37	1.79	12,200	4600	2.75	0.56	1.23	<0.05	828
Monitoring wells around the non-alkaline lake																			
MW04	6.79	1.29	-122	-2.09	-20.2	1.93	14.7	12.1	0.11	0.44	<0.03	0.04	644	158	38.5	0.95	9.99	<0.05	62.7
MW05A	6.32	0.70	-43.0	-2.01	-19.6	2.39	8.46	1.49	0.08	0.33	0.04	<0.015	366	84.6	25.5	1.94	4.00	<0.05	36.8
MW05B	6.54	0.67	-30.0	-1.64	-17.5	2.77	6.89	1.31	0.11	0.19	0.14	<0.015	379	89.1	17.3	3.96	9.31	<0.05	31.5
MW06A	6.76	1.11	-208	-3.86	-29.0	1.51	8.75	2.29	0.05	0.64	<0.03	0.02	513	115	33.7	3.52	6.54	<0.05	53.5
MW06B	6.74	0.58	-52.0	-2.96	-24.2	2.22	6.74	2.55	<0.015	0.09	<0.03	<0.015	572	124	39.9	3.01	9.97	<0.05	51.0
MW08	7.05	0.18	84.0	-2.41	-21.2	2.53	21.4	10.6	0.07	0.08	<0.03	0.05	991	207	105	0.29	15.4	<0.05	58.3
Monitoring wells in the sand hill																			
CD1	6.39	0.22	-54.0	-4.33	-31.3	1.63	6.05	1.25	0.15	0.07	<0.03	<0.015	84.3	8.34	3.95	17.3	1.04	0.9	8.46
CD2	6.16	0.20	-10.0	-1.47	-18.0	1.38	13.8	3.71	0.14	0.05	<0.03	0.02	61.6	9.09	4.78	8.35	2.04	0.63	12.1

Table 2 (continued)

Monitoring well	pH	EC mS cm ⁻¹	Eh mV	δ ¹⁸ O ‰	δ ² H ‰	DO mg L ⁻¹	Cl ⁻	SO ₄ ²⁻	NO ₃ ⁻	PO ₄ ³⁻	F ⁻	Br ⁻	HCO ₃ ⁻	Na ⁺	Ca ²⁺	Fe ²⁺	Mg ²⁺	Al ³⁺	K ⁺	
MW12	5.61	0.02	287	-6.17	-39.1	5.45	9.79	3.22	0.11	0.31	<0.03	<0.015	0.00	0.47	1.38	0.19	1.50	<0.05	2.38	
Alkaline-saline lake surface water																				
SW	9.23	3.50	130	0.98	-16.5	5.89	60.7	6.71	0.107	0.319	<0.03	0.148	1810	609	2.29	0	1.07	0.919	188	
Rain water																				
Dec. 2014	NA	NA	NA	-8.65	-60.2	NA	NA	NA	NA	NA	NA	NA	NA	NA	NA	NA	NA	NA	NA	NA
Jan. 2015	NA	NA	NA	-1.67	-11.0	NA	NA	NA	NA	NA	NA	NA	NA	NA	NA	NA	NA	NA	NA	NA
Feb. 2015	NA	NA	NA	-7.98	-58.9	NA	NA	NA	NA	NA	NA	NA	NA	NA	NA	NA	NA	NA	NA	NA
Mar. 2015	NA	NA	NA	-2.70	-26.3	NA	NA	NA	NA	NA	NA	NA	NA	NA	NA	NA	NA	NA	NA	NA

SW surface water, NA not analyzed, HCO₃⁻ estimated based on ionic balance

alkaline-saline lakes, where the pH is commonly higher than 9 (Furquim et al. 2008), albite and microcline have high rates of dissolution, liberating ions to the soils' solution (Brady and Walther 1989; Hellman 1994; Knauss and Copenhaver 1995).

The oversaturation of ions during the evaporative concentration in and around the lake depression has triggered the formation of mineral phases in the clay fraction of the soils, such as the precipitation directly from the lake of Mg-smectites (stevensite and saponite-like) into the H horizon, the precipitation of Ca and/or Mg carbonates (calcite, dolomite), the subsurface grayish Bkg horizon and the precipitation from the soil solution of Fe-micas (Fe-illite and glauconite) in the subsurface greenish and low-K horizon (Bnq) (Furquim et al. 2010a, b; Barbiero et al. 2017). Minor amounts of evaporite minerals (possibly nahcolite, thenardite, epsomite, mirabilite, halite, gypsum) can be observed on the lake bed during the dry season. Thus, the relative lowest concentrations of Ca²⁺, Mg²⁺ and Fe²⁺ in the alkaline-saline lake could be due to the involvement of these ions in the precipitation of silicate, carbonate and, to a lesser extent, evaporite minerals in and around the lake (Barbiero et al. 2002; Furquim et al. 2010a).

The significantly higher Fe²⁺ concentrations in the sand hill could be caused by Fe-bearing minerals' dissolution in acidic environment, associated with changes in the redox conditions promoted by water table oscillations. Remains of a degraded Bnq were observed by Barbiero et al. (2008) in deep positions of the same sand hill studied in this research, suggesting that the Fe-micas that accounts for most of the clay minerals of this horizon has been transformed in lower pH conditions, liberating Fe to the solutions. Summarizing, the chemistry data shows no evidence of significant contribution of the saline-alkaline water to the downgradient groundwater chemical composition.

The sources of water for groundwater and lakes and the role of evaporation and dissolution of salts in the salinity of the groundwater will be examined using the stable isotopes and Cl⁻ data in the next section.

Water isotopic composition

The stable isotope data for groundwater and surface water show a range of values that varied between -4.1 and +14.7‰ and -30.9 and +71‰ for δ¹⁸O and δ²H, respectively, during the dry season (Table 2). During the wet season, the range varied between -6.1 and 0.98‰ and -39 and -16.5‰ for δ¹⁸O and δ²H, respectively. The rain water showed a range of values between -8.65 and -1.67‰ and -11.03 and -60.23‰ for δ¹⁸O and δ²H, respectively. The isotope data is plotted in Fig. 5 using the global meteoric water line (GMWL) as a reference. The rain data should be plotted on top of the GMWL, and then the local meteoric

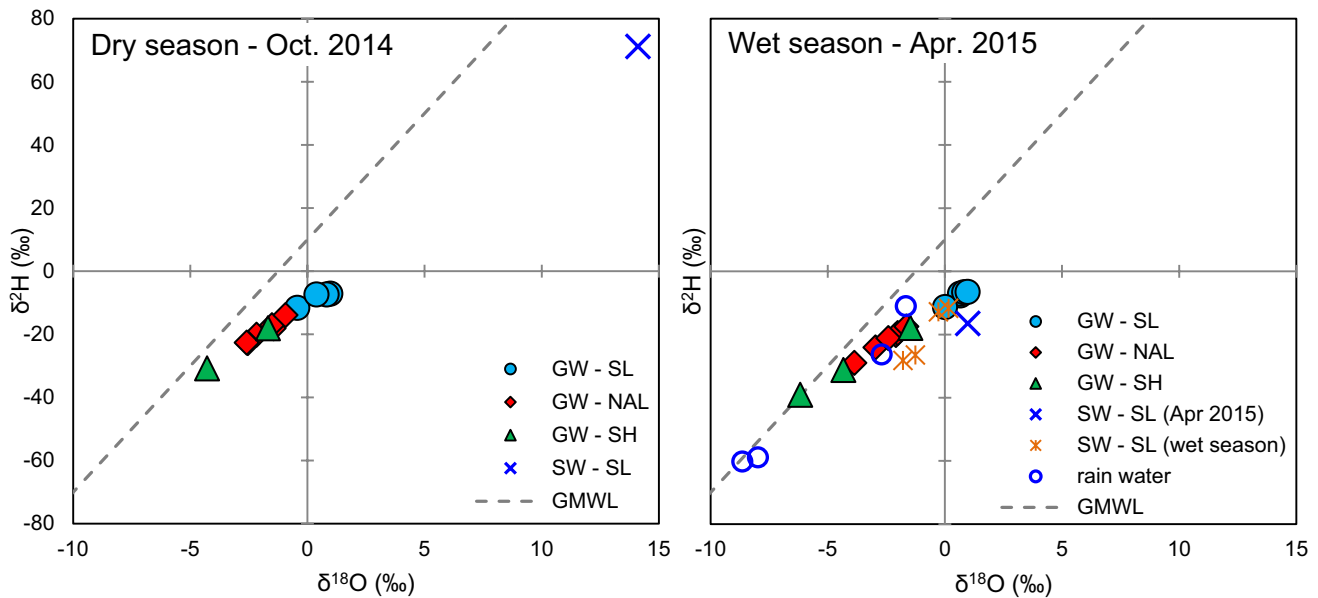


Fig. 5 Groundwater (GW), surface water (SW) and rainwater isotopic composition during the wet and dry seasons; *GMWL* global meteoric water line. Rainwater and SW–SL include results from Dec. 14 to Mar. 15

water line should be like the *GMWL*. The isotope data showed a trend away from the global meteoric water line, which is typical of water affected by evaporation (Clark and Fritz 1997). The groundwater in the alkaline–saline lake area is more enriched isotopically than the groundwater in the non-saline lake area. The intersect of the evaporation line with the *GMWL* corresponds to the isotopic composition of the precipitation which is the source of recharge to groundwater and lakes in the study area. The groundwater in the sand hill area, since it is not affected by evaporation, represents the isotope composition of the recharge water in the study area. In the dry season, the alkaline–saline lake surface water was much more isotopically enriched in comparison to all groundwater samples, likely caused by significant evaporation of the surface water (Table 2). The surface water $\delta^{18}\text{O}$ and $\delta^2\text{H}$ enrichment in 16 alkaline–saline lakes in Nhecolândia due to evaporation was also described by Almeida et al. (2010). The $\delta^{18}\text{O}$ and $\delta^2\text{H}$ values determined for the surface water in the dry season in this study are above the average values determined for hypersaline lakes in Almeida et al. (2010).

The groundwater isotope signature in the alkaline lake area did not change significantly between the dry and wet seasons, but the alkaline–saline lake surface water became more isotopically depleted in the wet season, even lower than the surrounding groundwater (Fig. 5). This confirms that the inflow to the alkaline–saline lake in the wet season was mainly by the more isotopically depleted rainwater (through direct precipitation, shallow subsurface flow and runoff), and not by the already isotopically enriched groundwater. The

groundwater in the alkaline–saline lake region was enriched in $\delta^{18}\text{O}$ and $\delta^2\text{H}$ in comparison to the groundwater in the sand hill and non-alkaline lake. This indicates that the surface water in the alkaline–saline lake is recharging the surrounding groundwater, consistently with the flow direction inferred from potentiometric measurements.

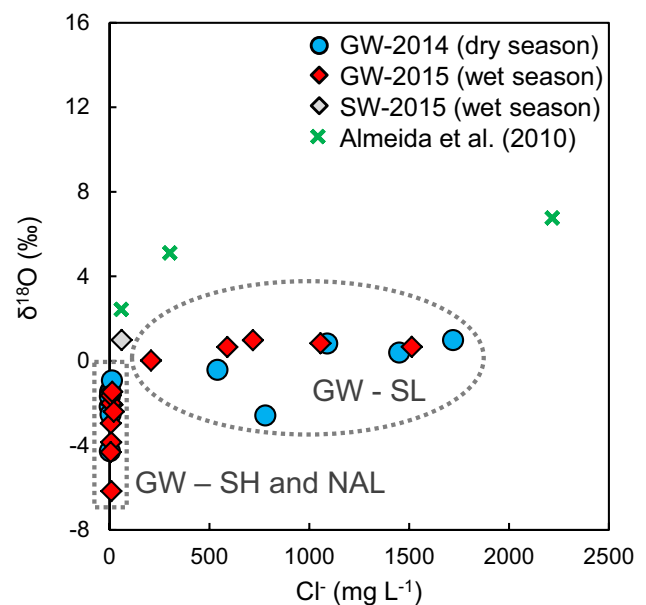


Fig. 6 Chloride versus $\delta^{18}\text{O}$ in groundwater (GW) and surface water (SW) around the alkaline–saline lake (SL), sand hill (SH) and non-alkaline lake (NAL)

The relation between Cl^- and $\delta^{18}\text{O}$ provides another evidence that groundwater does not recharge the alkaline–saline lake (Fig. 6). If groundwater was recharging the alkaline–saline lake, Cl^- concentrations in the lake water should be in the same order of magnitude (in the wet season) or greater (in the dry season) than the values observed in the groundwater around the alkaline–saline lake. When comparing the groundwater results with values from saline lakes from other studies in which higher Cl^- concentrations were measured, the Cl^- concentrations are usually below the values measured in groundwater, being slightly greater only for the hypersaline lake (Almeida et al. 2010) (Fig. 6). In addition, Cl^- concentrations in the groundwater increase without any change in the isotopic composition, reflecting an interaction of the water with saline sediments in the lake bed, as the water slowly infiltrates through this low-K layer. The high groundwater salinity is therefore associated with evaporation plus dissolution of salts during infiltration of the lake water.

The isotopically enriched and high ion concentration groundwater surrounding the saline lake does not appear to have a significant flow away from the lake, since there is an abrupt decrease in ions' concentration and change in isotopic composition compared to the groundwater in the sand hill. Despite the occurrence of a hydraulic gradient, the low-K layer (Bnq horizon) likely acts as a barrier to groundwater flow. Therefore, the relatively small extension of the enriched and high EC groundwater is likely due to a small fraction of enriched groundwater mixing with groundwater from other recharge zones less impacted by evaporation, such as depressions like the non-alkaline lake. Also, the higher EC groundwater has higher density compared to the surrounding groundwater. According to Post (2012), groundwater with EC around 20 mS cm^{-1} , would have a density approximately 1% higher. The density contrast between the high EC water and the fresh groundwater could cause it to sink, resulting in higher EC (and ions' concentration) at greater depths. This was observed at the multilevel well MW02, which had 20–40% higher EC values in the deeper level, despite the relatively low vertical distance between them (only 0.3 m). Therefore, the enriched, high EC groundwater tends to flow downwards and is not found in shallow wells more distant to the alkaline–saline lake.

Integrated conceptual model for groundwater–surface water interaction

According to water elevation and chemical data during the period of this study, the alkaline–saline lake receives inflow during the wet season through direct precipitation, runoff and shallow subsurface flow and the water is retained in the lake throughout the whole year. During the dry season, significant evaporation occurs which results in higher EC

and isotopic enrichment in the surface water, and significant reduction in the lake surface area. Due to this permanent water accumulation at relatively high elevation, the alkaline–saline lake acts as a recharge zone to the surrounding groundwater during the whole year. The lake isotopically enriched and ion-concentrated water slowly percolates through the low permeability soils, possibly dissolving some minerals, with the consequent increase in some ions' concentration in groundwater around the lake. Due to a low-K horizon (Bnq) in the alkaline–saline lake surroundings, groundwater flow is limited, and the enriched groundwater does not travel at a significant flow rate. Therefore, the groundwater in the sand hill and in proximity to the non-alkaline lake is characterized by more depleted isotopic composition and lower ions' concentration. A summary of the site conceptual model is presented in Fig. 7.

Evidence of groundwater recharge from the alkaline–saline lakes in this study disagrees with the studies by Barbiero et al. (2008) and Furian et al. (2013), which proposed that the alkaline–saline lakes received groundwater during the wet season and remained isolated from groundwater during the dry season. Barbiero et al. (2008) indicated that only in short periods, corresponding to the beginning of the wet season, flow occurred from the alkaline–saline to the non-alkaline lakes. Based on data collected from 1998 to 2002, Barbiero et al. (2008) concluded that in the wet season, groundwater flow would occur from the non-saline lake to the alkaline–saline lake, where it evaporates. In contrast, our study shows that the flow system does not connect the two lakes.

In the study site, the alkaline–saline lake acts as a local recharge zone, but the non-alkaline lakes and other depressions also are recharge zones. The groundwater recharge in topographical lows, as supported by the potentiometric, chemical and isotopic data of this research, is known in the literature as depression-focused recharge, a process that is concentrated in small areas of the landscape (e.g., ponds, lakes) (Lissey 1971; Winter 1999). It has been described in the North America prairies (Berthold et al. 2004; Delin et al. 2000), sand dunes (Jacks and Traoré 2014) and coastal areas (Logan and Rudolph 1997; Phillips and Shedlock 1993). All the regions marked by the domain of this type of recharge have a significant annual water deficit, in which the evapotranspiration exceeds the precipitation rates, condition that prevents the development of integrated drainage networks at least part of the year. Also, they are all in nearly flat terrains punctuated by small and shallow depressions, characterizing a hummocky landscape.

The Nhecolândia fulfills these environmental conditions, with an annual hydrological deficit of 300 mm (Alfonsi and Camargo 1986; Por 1995), sufficient for the seasonal development of intermittent watercourses between the non-alkaline lakes, and very low slope gradients (< 1%) (Silva 1986),

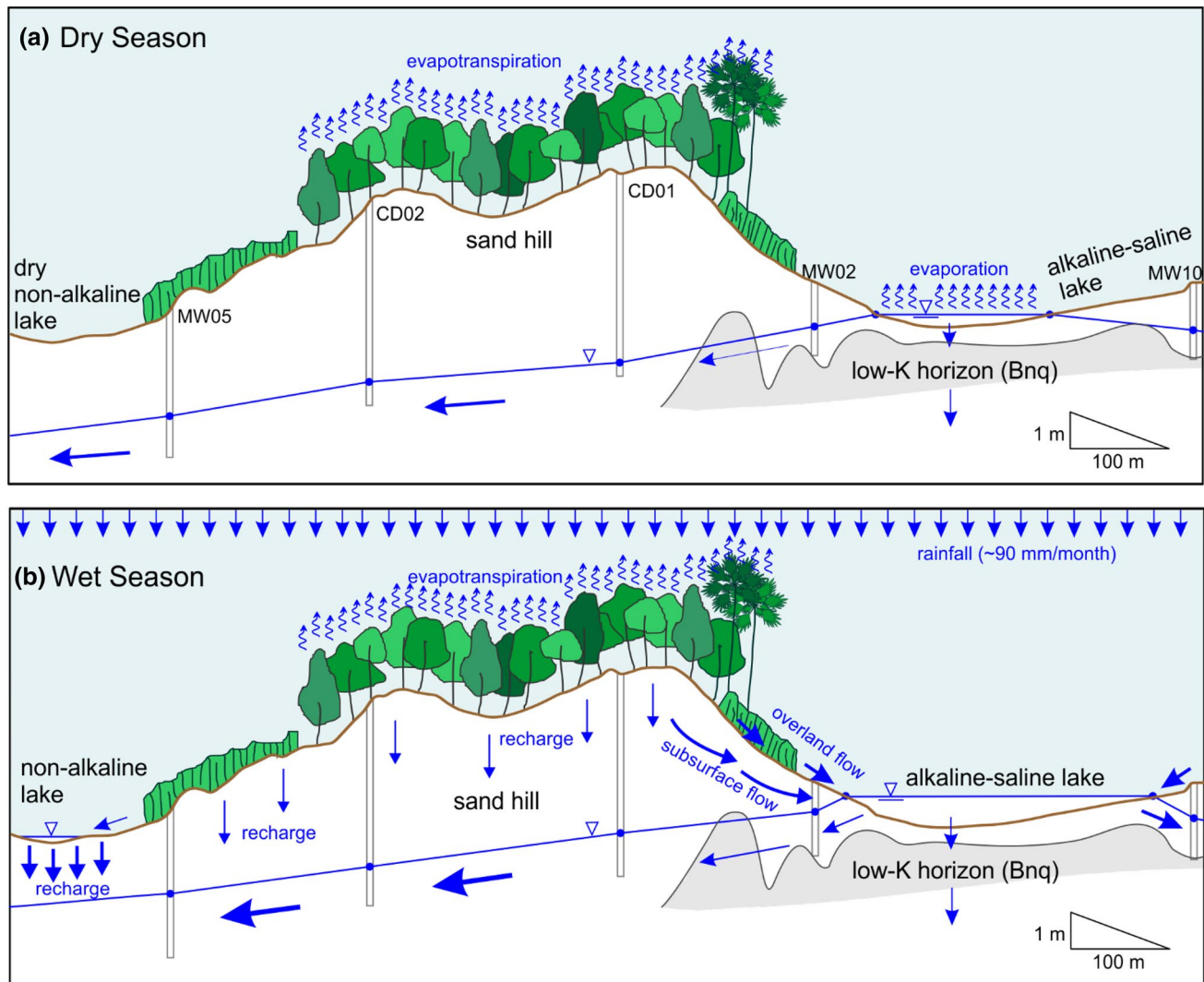


Fig. 7 Site hydrologic conceptual model for the dry (a) and wet seasons (b). Adapted from: Barbiero et al. (2008); Zevenbergen (2012)

with a local altitudinal difference of about 5 m between the bottom of the depressions and the top of the sand hills. Thus, the subregion has the requirements for the development of depression-focused recharge, which is likely occurring in all its topographical lows, including small ponds, as observed by Furian et al. (2013), and the alkaline–saline and non-alkaline lakes, as described in the present work.

The recharge in the highest areas of the landscapes (sand hills), as suggested by Costa et al. (2015), was not high enough to promote a reversal in flow direction (towards the alkaline–saline lake) and possibly was limited because of the high evapotranspiration rates, promoted by the dense forested savanna vegetation of the sand hills (Zevenbergen 2012), in contrast to the bare soil around the alkaline–saline lakes and the open grass savanna of the non-alkaline lakes and ponds. Oliveira et al. (2017), considering different physiognomies of the Brazilian savanna, also showed a decrease

in the groundwater recharge from the grassland to the woodland, reflecting the higher evapotranspiration rates of denser vegetation.

Conclusions

In the Nhecolândia region of the Pantanal wetland, there are lakes closely located with very contrasting surface water properties, namely the alkaline–saline lakes and non-alkaline lakes. The study of hydraulic heads, chemical and isotopic water composition coupled with pedological evidence provided insights on the interaction between groundwater and the surface water from the different lake types.

Contrary to conceptual site models presented in the literature (Barbiero et al. 2008; Costa et al. 2015), this study indicated that the alkaline–saline lake does not receive

groundwater inflow. The surface water elevation was higher than the hydraulic heads in the surrounding groundwater, and mini-piezometers installed in the studied alkaline–saline lake bed and in two additional alkaline–saline lakes indicated downward flow direction. In the dry season, the alkaline–saline lake surface water was isotopically enriched in ^{18}O and ^2H due to evaporation but became isotopically depleted in the wet season due to the input of rain water. The groundwater in the wells surrounding the alkaline saline lake was isotopically enriched in comparison to the groundwater from other locations, indicative of recharge with the alkaline–saline lake-enriched water. The water chemical composition also provided evidence that the alkaline–saline lake is a recharge zone. Higher Na^+ and Cl^- concentrations were found in the groundwater in comparison to the surface water and there was no correlation between Cl^- and $\delta^{18}\text{O}$ in the groundwater, indicative of Cl^- concentrations being controlled by water interaction with lakebed sediments as the water slowly infiltrates.

The enriched and high ion concentration groundwater is found only close to the alkaline–saline lake, likely because a low-K layer (Bnq) below the lakebed does not allow a significant groundwater flow to downgradient regions. This also allows water retention in the lake even during the dry season, when significant evaporation occurs. The evaporation results in a distinct composition in the alkaline–saline lake surface water and surrounding groundwater in comparison to groundwater in the sand hill and non-alkaline lake surroundings. This disconnection between the groundwater surrounding the alkaline–saline lake and the groundwater in the sand hill and non-alkaline lake contrasts with the conceptual model presented in other studies (Barbiero et al. 2008), in which flow was described to occur from the non-alkaline lake to the alkaline–saline lake.

The general groundwater flow direction is from NNW to SSE but can have some local changes during the wet season due to recharge in depressions such as the non-alkaline lake, which acts as a recharge zone during the wet season, when it accumulates water. The same appears to occur in other depressions in the area, in a behavior typical of depression-focused recharge zones, where the depressions act as recharge zones during precipitation events.

Acknowledgements The authors would like to thank the support from Empresa Brasileira de Pesquisas Agropecuárias (EMBRAPA Pantanal) and the financial support from FAPESP (2011/22491-0). We also thank INCT de Estudos do Meio Ambiente (INCT-EMA) (CNPq: 703905/2009 and FAPESP: 2008/57708-7) and Centro Cooperativo de Engenharia Ambiental (CEPEMA) (Processo FAPESP: 2013/50218-2).

References

- Alfonsi RR, Camargo MBP (1986) Condições climáticas para a região do Pantanal Matogrossense. In: Anais do 1° Simpósio sobre Recursos Naturais e Sócio-Econômicos do Pantanal. Corumbá (MS), Brazil, pp 29–42
- Almeida TIR, Sígolo JB, Fernandes E, Queiroz Neto JP, Barbiero L, Sakamoto AY (2003) Proposta de Classificação e Gênese das Lagoas da Baixa Nhecolândia—MS com Base em Sensoriamento Remoto. *Revista Brasileira de Geociências* 33:83–90
- Almeida TIR, Karmann I, Paranhos Filho ACP, Sígolo JB, Bertolo RA (2010) Os diferentes graus de isolamento da água subterrânea como origem de sua variabilidade: evidências isotópicas, hidroquímicas e da variação sazonal do nível da água no Pantanal da Nhecolândia. *Geologia USP Série Científica* 10:37–47
- Alvarenga SM, Brasil AE, Pinheiro R, Kux HJH (1984) Estudo Geomorfológico Aplicado à Bacia do Alto Rio Paraguai e Pantanaís Matogrossenses. *Boletim Técnico Projeto Radambrasil* 1:187
- Assine ML (2003) Sedimentação na Bacia do Pantanal Mato-Grossense, Centro-Oeste do Brasil. Tese de Livre-Docência, UNESP, Instituto de Geociências e Ciências Exatas, Rio Claro, p 106
- Assine ML, Merino ER, Pupim FP, Macedo HA, Santos MGM (2015) The Quaternary alluvial systems tract of the Pantanal Basin, Brazil. *Braz J Geol* 45:475–489
- Barbiero L, Queiroz Neto JP, Ciornei G, Sakamoto AY, Capellari B, Fernandes E, Valles V (2002) Geochemistry of water and ground water in the Nhecolândia, Pantanal of Mato Grosso, Brazil: variability and associated processes. *Wetlands* 22(3):528–540
- Barbiero L, Rezende Filho A, Furquim SAC, Furian S, Sakamoto AY, Valles V, Graham RC, Fort M, Ferreira RPD, Queiroz Neto JP (2008) Soil morphological control on saline and freshwater lake hydrogeochemistry in the Pantanal of Nhecolândia, Brazil. *Geoderma* 148(1):91–106
- Barbiero L, Berger G, Filho ATR, Meunier JF, Martins-Silva ER, Furian S (2017) Organic Control of dioctahedral and trioctahedral clay formation in an alkaline soil system in the Pantanal Wetland of Nhecolândia, Brazil. *PLoS One* 11(7):1–23
- Barbiero L, Siqueira Neto M, Braz RR, Carmo JB, Rezende Filho AT, Mazzi E, Fernandes FA, Damato SR, Camargo PB (2018) Biogeochemical diversity, O_2 -supersaturation and hot moments of GHG emissions from shallow alkaline lakes in the Pantanal of Nhecolândia, Brazil. *Sci Total Environ* 619–620:1420–1430
- Berbery EH, Barros VR (2002) The hydrologic cycle of the La Plata Basin in South America. *J Hydrometeorol* 3:630–645
- Berthold S, Bentley LR, Hayashi M (2004) Integrated hydrogeological and geophysical study of depression-focused groundwater recharge in the Canadian prairies. *Water Resour Res* 40:1–14
- Bradley C, Baker A, Cumberland S, Boomer I, Morrissey IP (2007) Dynamics of water movement and trends in dissolved carbon in a headwater wetland in a permeable catchment. *Wetlands* 27(4):1066–1080
- Brady PV, Walther JV (1989) Controls on silicate dissolution rates in neutral and basic pH solutions at 25 °C. *Geochim Cosmochim Acta* 53:2823–2830
- Capellari B (2001) Sensoriamento remoto aplicado ao estudo da dinâmica hidrológica da região da Nhecolândia, Pantanal Matogrossense, MS. Dissertação de Mestrado, Universidade de São Paulo-USP, Departamento de Geografia, p 100
- Carvalho N (1986) Hidrologia da Bacia do Alto Paraguai. In: Anais do 1° Simpósio sobre Recursos Naturais e Sócio-Econômicos do Pantanal. Corumbá (MS), Brazil, pp 43–49
- Clark ID, Fritz P (1997) Environmental isotopes in hydrogeology. CRC Press, Boca Raton, p 328
- Collischonn W, Tucci CEM, Clarke RT (2001) Further evidence of changes in the hydrological regime of the River Paraguay: part of a wider phenomenon of climate change? *J Hydrol* 245:218–238
- Cordeiro NV (1999) Environmental management issues in the Plata basin. In: Biswas AK, Cordeiro NC, Braga BPF, Tortajada C (eds) Management of Latin America river basins: Amazon,

- Plata and São Francisco. Water Resources Management and Policy Series Editors, New York, pp 148–173
- Costa M, Telmer KH, Evans TL, Almeida TI, Diakun MT (2015) The lakes of the Pantanal: inventory, distribution, geochemistry, and surrounding landscape. *Wetl Ecol Manag* 23(1):19–39
- Del'Arco JO, Silva RH, Tarapanoff I, Freire FA, Pereira LGM, Souza SL, Luz DS, Palmeira RCB, Tassinari CCG (1982) Geologia da Folha SE.21-Corumbá e Parte da Folha SE.20. In: RADAM-BRASIL-Levantamento dos Recursos Naturais. Rio de Janeiro, pp 25–160
- Delin GN, Healy RW, Landon MK, Bohlke K (2000) Effects of topography and soils properties on recharge at two sites in an agricultural field. *J Am Water Resour Assoc* 36(6):1401–1416
- Evans TL, Costa M (2013) Landcover classification of the lower Nhecolândia subregion of the Brazilian Pantanal wetland using ALOS/PALSAR, RADARSAT-2 and NVISAT/ASAR imagery. *Remote Sens Environ* 128:118–127
- FAO—Food and Agriculture Organization of the United Nation (2016) La Plata Basin. AQUASTAT database. <http://www.fao.org/nr/water/aquastat/basins/la-plata/index.stm>. Accessed May 2017
- Fernandes E, Sakamoto AY, Queiroz Neto JP, Lucati HM, Capellari B (1999) Le Pantanal da Nhecolândia, Mato Grosso: cadre physique et dynamique hydrologique. *Geografia Física e Dinamica Quaternaria* 22:13–21
- Furian S, Martins ERC, Parizotto MT, Rezende Filho A, Victoria RL, Barbiero L (2013) Chemical diversity and spatial variability in myriad lakes in Nhecolândia in the Pantanal wetlands of Brazil. *Limnol Oceanogr* 58(6):2249–2261
- Furquim SAC (2007) Formação de Carbonatos e Argilominerais em Solos Sódicos no Pantanal Sul-Mato-Grossense. Tese de Doutorado, Universidade de São Paulo (USP), Departamento de Geografia
- Furquim SAC, Graham R, Barbiéro L, Queiroz Neto JP, Vallès V (2008) Mineralogy and genesis of smectites in an alkaline-saline environment of Pantanal wetland, Brazil. *Clays Clay Miner* 56:580–596
- Furquim SAC, Graham RC, Queiroz Neto BL, Vidal-Torrado JP P (2010a) Soil mineral genesis and distribution in a saline lake landscape of the Pantanal Wetland, Brazil. *Geoderma* 154:518–528
- Furquim SAC, Barbiéro L, Graham RC, Queiroz Neto JP, Dias Ferreira RP, Furian S (2010b) Neof ormation of micas in soils surrounding an alkaline-saline lake of Pantanal wetland, Brazil. *Geoderma* 158:331–342
- Godoi Filho JD (1986) Aspectos Geológicos do Pantanal Mato-grossense e de sua Área de Influência. In: Anais do 1º Simpósio sobre Recursos Naturais e Sócio-Econômicos do Pantanal. Corumbá (MS), Brazil, pp 63–76
- Google Earth 7.3.2 (2017) [Aerial image of Pantanal wetland, Brazil; coordinates 18°58'27.59" S and 56°38'51.01" O]. Retrieved August 2 2017
- Hamilton SK (1999) Potential effects of a major navigation project (Paraguay-Paraná Hidrovía) on inundation in the Pantanal floodplains. *Regul Rivers Res Manag* 15:289–299
- Hamilton SK, Sippel SJ, Melack JM (1996) Inundation patterns in the Pantanal wetland of South America determined from passive microwave remote sensing. *Arch Hydrobiol* 137(1):1–23
- Hamilton SK, Sippel SJ, Melack JM (2002) Comparison of inundation patterns among major South American floodplains. *J Geophys Res* 107:1–14
- Hellman R (1994) The albite-water system: part I. The kinetics of dissolution as a function of pH at 100, 200, and 300 °C. *Geochim Cosmochim Acta* 58:595–611
- Jacks G, Traoré MS (2014) Mechanisms and rates of groundwater recharge at Timbuktu, Republic of Mali. *J Hydrol Eng* 19(2):422–427
- Junk WJ, Cunha CN, Wantzen KM, Petermann P, Strussmann C, Marques MI, Adis J (2006) Biodiversity and its conservation in the Pantanal of Mato Grosso, Brazil. *Aquat Sci* 68:278–309
- Kebede S, Abdalla O, Sefelnasr A, Tindimugaya C, Mustafa O (2016) Interaction of surface water and groundwater in the Nile River basin: isotopic and piezometric evidence. *Hydrogeol J* 25(3):1–20
- Knauss KG, Copenhaver SA (1995) The effect of malonate on the dissolution kinetics of albite, quartz, and microcline as a function of pH at 70 °C. *Appl Geochem* 10:17–33
- Lee DR, Cherry JA (1978) A field exercise on groundwater flow using seepage meter and mini-piezometers. *J Geol Educ* 27:6–9
- Lissey A (1971) Depression-focused transient groundwater flow patterns in Manitoba. *Geol Assoc Can Spec Pap* 9:333–341
- Logan WS, Rudolph DL (1997) Microdepression-focused recharge in a coastal wetland, La Plata, Argentina. *J Hydrol* 194:221–238
- Montalván FJ, Heredia J, Ruiz JM, Pardo-Igúzquiza E, García de Domingo A, Elorza FJ (2017) Hydrochemical and isotopes studies in a hypersaline wetland to define the hydrogeological conceptual model: Fuente de Piedra Lake (Malaga, Spain). *Sci Total Environ* 576:335–346
- OEA—Organización de los Estados Americanos (2017) Análisis Diagnóstico Transfronterizo de la Cuenca del Plata-ADT. Ciudad Autónoma de Buenos Aires: Comité Intergubernamental Coordinador de los Países de la Cuenca del Plata-CIC
- Oliveira PTS, Leite MB, Mattos T, Nearing MA, Scott RL, Xavier RO, Matos DMS, Wendland E (2017) Groundwater recharge decrease with increased vegetation density in the Brazilian cerrado. *Ecohydrol* 10:1–8
- Padovani CR (2010) Dinâmica espaço-temporal das inundações no Pantanal. Tese de Doutorado, Universidade de São Paulo (USP), Escola Superior de Agricultura Luiz de Queiroz (Esalq), p 174
- Phillips PJ, Shedlock RJ (1993) Hydrology and chemistry of groundwater and seasonal ponds in the Atlantic Coastal Plain in Delaware, USA. *J Hydrol* 141:157–178
- Por FD (1995) The Pantanal of Mato Grosso (Brazil)—world's largest wetland. Kluwer Academic Publishers, Dordrecht, p 122
- Post VEA (2012) Electrical conductivity as a proxy for groundwater density in coastal aquifers. *Ground Water* 50(5):785–792
- Rosenberry DO, Lewandowski J, Meinikmann K, Nützmann G (2015) Groundwater—the disregarded component in lake water and nutrient budgets. Part 1: effects of groundwater on hydrology. *Hydrol Process* 29(13):2895–2921
- Schoeneberger PJ, Wysocki DA, Benham EC, Soil Survey Staff (2012) Field book for describing and sampling soils, Version 3.0. Natural Resources Conservation Service, National Soil Survey Center, Lincoln
- Scott DA (1991) Latin America and the Caribbean. In: Finlayson CM, Moser ME (eds) *Wetlands: a global perspective*. Facts on File, New York, pp 85–114
- Silva TC (1986) Contribuição da Geomorfologia para o Conhecimento e Valorização do Pantanal. In: Anais do 1º Simpósio sobre Recursos Naturais e Sócio-Econômicos do Pantanal, Corumbá (MS), Brazil, pp 77–90
- Silva CJ, Wantzen KM, Nunes da Cunha C, Machado FDA (2001) Biodiversity in the Pantanal Wetland, Brazil. In: Gopal B, Junk WJ, Davis JA (eds) *Biodiversity in wetlands: assessment, function and conservation*, vol 2. Backhuys Publishers, Leiden, pp 187–215
- USEPA (1999) Method 300.1—determination of inorganic ions in drinking water by ion chromatography. Revision 1.0
- USEPA (2007) Method 3015A—microwave assisted acid digestion of aqueous samples and extracts. Revision 1
- Winter TC (1999) Relation of streams, lakes, and wetlands to groundwater flow systems. *Hydrogeol J* 7:28–45
- Zani H, Assine ML, Araújo BC, Merino ER, Silva A, Fanciani EM (2006) Lobos deposicionais na evolução do megaleque do rio Taquari, Pantanal Mato-grossense. In: Anais do 1º Simpósio de

Geotecnologias no Pantanal, Embrapa Informática Agropecuária/INPE, p 285–292

Zani H, Assine ML, McGlue MM (2012) Remote sensing analysis of depositional landforms in alluvial settings: method development and application to the Taquari megafan, Pantanal (Brazil). *Geomorphology* 161–162:82–92

Zevenbergen AF (2012) A modelling study on the effect of groundwater on vegetation and the effect of vegetation on groundwater

in the Pantanal of Mato Grosso, Brazil. MSc Thesis, University of Utrecht

Publisher's Note Springer Nature remains neutral with regard to jurisdictional claims in published maps and institutional affiliations.